# Dual-State Emissive π-Extended Salicylaldehyde Fluorophores: Synthesis, Photophysical Properties and First-Principle Calculations

Timothée Stoerkler, Denis Frath, Denis Jacquemin, Julien Massue, Gilles Ulrich

# Dual-State Emissive π-Extended Salicylaldehyde Fluorophores: Synthesis, Photophysical Properties and First-Principle Calculations

Timothée Stoerkler,[†] Denis Frath,[†] Denis Jacquemin,[*‡] Julien Massue[*†] and Gilles Ulrich[*†]

[†] Institut de Chimie et Procédés pour l'Energie, l'Environnement et la Santé (ICPEES), Equipe Chimie Organique pour la Biologie, les Matériaux et l'Optique (COMBO), UMR CNRS 7515, Ecole Européenne de Chimie, Polymères et Matériaux (ECPM), 25 Rue Becquerel, 67087 Strasbourg Cedex 02, France

[‡] CEISAM Lab-UMR 6230-CNRS and University of Nantes, Nantes, France

Emails: Denis.Jacquemin@univ-nantes.fr, massue@unistra.fr, gulrich@unistra.fr

## Abstract

The search for simple, low-cost, versatile, easily accessible, stimuli-responsive, highly emissive molecular fluorophores emitting both in solution and in the solid-state has prompted us to investigate the optical properties of a series of synthetically accessible salicyladehyde derivatives possessing a π-conjugated moiety at their 4-position. These dyes are mainly known as synthetic intermediates but can also display sizeable Excited-State Intramolecular Proton Transfer (ESIPT) fluorescence owing to the presence of a 6-membered H-bonded ring in their structure. The photophysical properties of these compounds have been studied in solution (multiple solvents) and in the solid-state, as doped in PMMA films, leading to the observation of a pronounced fluorosolvatochromism. Modification of the spacer (ethynyl, vinyl or direct connection) involved the π-delocalization triggers major differences in terms of maximum emission wavelength and fluorescence quantum yields in the various media studied. All photophysical observations are rationalized by first-principle calculations.

## Introduction

Functional fluorescent emitters based on a rationally (poly)substituted organic π-conjugated scaffold have found applications in cutting-edge innovations in a wide range of fields owing to their synthetic availability, modularity, absence of toxicity, non-invasiveness, low-cost, up scalability, and industrial processability.[1] Molecular fluorophores encompass several families of well-known dyes including fluorescent heterocyclic architectures derived from cyanines,[2] rhodamines,[3] squaraines[4] or boron complexes,[5] just to name a few. Although highly emissive in solution and presenting tunable fluorescence wavelengths, the majority of the dyes reported so far are however heavily quenched in the solid-state due to detrimental aggregation processes, generally called aggregation-caused quenching (ACQ) effects. In the same time, aggregation-induced emission (AIE) dyes have been engineered with the view to compensate for this drawback and deliver rotors-shaped emitters with strong fluorescence intensity at high concentrations in solution or in confined matrixes like nanoparticles.[6] Dual-state emitters (DSE) have been developed more recently and originate from a rational design allowing the observation of fluorescence emission both in solution and in the solid-state.[7] These innovative probes arise from a tenuous balance between molecular rigidity, quasi-planarity and the introduction of appropriate solubilizing entities. There are no established general rules to engineer DSE probes but a strong lack of molecular symmetry is usually observed to entail DSE emission among these dyes. Recent examples including imidazo[1,2-f]phenanthridine,[8] 2,5-dithienylpyrrole,[9] 2-(2'-hydroxyphenyl)benzimidazole,[10] among others[11] have opened up the possibility to interlink applications usually targeted by traditional fluorophores, *i.e.*, dyes emitting in solution and solid-state dyes, including AIE probes. The search for original structures displaying DSE properties is strongly pursued by heterocyclic chemists due to the imperious necessity to elaborate design rules as well as to reach overall disruptive progress in the field of organic dyes.

Salicylaldehyde derivatives are synthetic intermediates widely reported in the literature as precursors for the elaboration of Schiff bases,[12] Salen-based probes[13] and other heterocycles.[14] They present with the advantage of being inexpensive commercially available reagents or obtainable in a limited number of synthetic steps. Moreover, a recent example pointed out the use of unsubstituted deprotonated salicylaldehyde as a photocatalyst relying on visible light.[15] However, unlike acetophenones or benzophenones analogs,[16] salicylaldehyde derivatives display reduced chelating ability toward metal or metalloid ions, unless an additional chelating group is inserted in the vincinity.[17] Nevertheless, some coordination complexes

involving salicyladehyde derivatives have been described.[18] Salicyladehydes derivatives typically display weak emission in solution due to the possibility of Excited-State Intramolecular Proton Transfer (ESIPT) emission, owing to the presence of 6-membered H-bonded ring.[19] ESIPT is a photophysical process, consisting of a phototautomerism that can be partially or fully frustrated depending on the position and nature of electronic substitution on the molecular scaffold.[20] During the course of previous studies, we serendipitously found that substitution at the 4-position of selected salicyaldehyde derivatives could trigger strong naked-eye fluorescence which prompted us to investigate more deeply the photophysical properties of salicyaldehydes functionalized at the *para* position with respect to the formyl group. The studies reported herein investigate the influence of the nature of the π-conjugated spacer and the electronic substitution on the optical properties of the resulting dyes. Three different spacers were considered: ethynyl, vinyl or a direct connection between salicylaldehyde and various aryl groups (Figure 1).

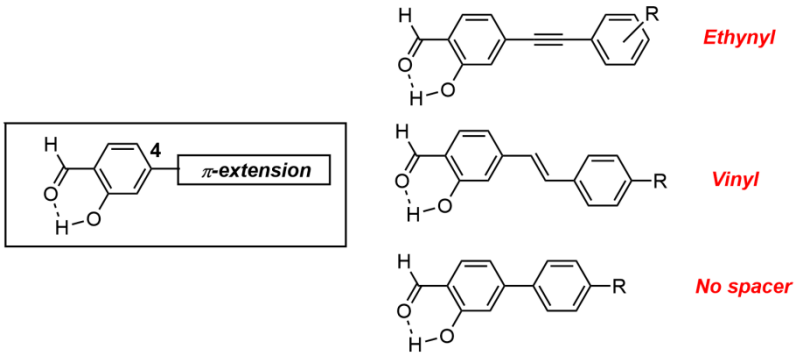


**Figure 1**. 4-extended salicylaldehyde derivatives reported herein.

## Synthesis

The synthesis of 4-extended salicylaldehydes **1a-d**, **2a-b** and **3a-b** is described on Scheme 1. Salicylaldehyde dyes **1a-d**, **2a-b** and **3a-b** were obtained in one step from commercially available 4-bromosalicylaldehyde, using classical Pd-catalyzed cross-coupling reactions, Sonogashira coupling for **1a-d**, Heck coupling for **2a-b** and Suzuki-Miyaura coupling for **3a-b**. Compounds **1a-d**, **2a-b** and **3a-b** were obtained as white to yellow powders or oil in 35-97% yield, after purification on a column chromatography. All new compounds were characterized by $^{1}H$ and $^{13}C$ NMR spectroscopy, as well as HR-MS spectrometry (see the SI).

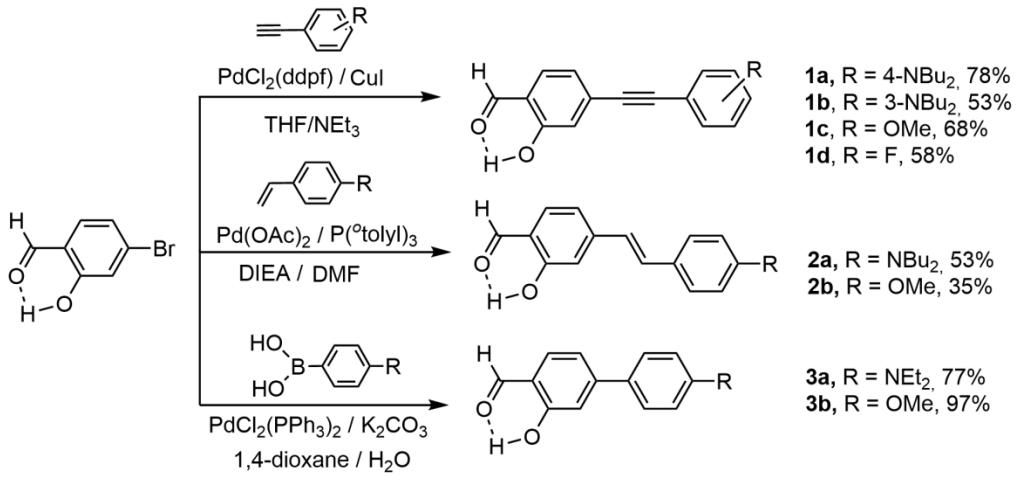


**Scheme 1**. Synthesis of 4-extended salicylaldehyde derivatives **1a-d**, **2a-b** and **3a-b**

## Experimental section

### Materials and methods

All chemicals were received from commercial sources (Sigma Aldrich, Fluorochem) and used without further purification. Tetrahydrofuran (THF) was distilled over metallic sodium (Na). Triethylamine ($NEt_3$) was distilled under argon over KOH. Thin layer chromatography (TLC) was performed on silica gel coated with fluorescent indicator. Chromatographic purifications were conducted using 40-63 μm silica gel.

$^1H$ NMR (500 MHz) and $^{13}C$ NMR (126 MHz) spectra were recorded on a Bruker Advance spectrometer with perdeuterated solvents containing residual protonated solvent signals as internal references. Absorption spectra were recorded using a dual-beam grating Schimadzu UV-3000 absorption spectrometer with a quartz cell of 1 cm of optical path length. The steady-state fluorescence emission and excitation spectra were recorded by using a Horiba S2 Jobin Yvon Fluoromax 4. All fluorescence and excitation spectra were corrected. Solvents used for spectroscopy were spectroscopic grade and were used as received.

The fluorescence quantum yields ($\Phi_{exp}$) were measured in diluted solutions with an absorption value below 0.1 at the excitation wavelength using the following equation:

$$\Phi_{exp} = \Phi_{ref} \frac{I}{I_{ref}} \frac{OD_{ref}}{OD} \frac{\eta^2}{\eta^2_{ref}} \quad (eq\ 1)$$

I is the integral of the corrected emission spectrum, OD is the optical density at the excitation wavelength, and η is the refractive index of the medium. The reference system used was Rhodamine 6G, Φ = 88% in ethanol ($\lambda_{exc}$ = 488 nm).

Luminescence lifetimes were measured on a Horiba Scientific TCSPC system equipped with a nanoLED 370. Lifetimes were deconvoluted with FS-900 software using a light-scattering solution (LUDOX) for instrument response. The excitation source was a laser diode ($\lambda_{exc}$ = 320 nm).

N,N-dibutyl-3-iodoaniline,[21] N,N-dibutyl-4-ethynylaniline[22] and salicylaldehyde **2a**[23] were synthesized according to reported procedures.

**N,N-dibutyl-3-trimethysilylethynylaniline**: To a solution of N,N-dibutyl-3-iodoaniline (1 mmol) in a mixture of THF/$NEt_3$ (20 mL/5 mL) was added $Pd(PPh_3)_2Cl_2$ (0.05 mmol). The resulting mixture was degassed with Ar 30 minutes before ethynyltrimethylsilane (3 mmol) and CuI (0.1 mmol) were added. The mixture which turned rapidly black was stirred overnight at 60°C. The solution was then taken up in $CH_2Cl_2$, washed with water three times, dried over $MgSO_4$ and concentrated *in vacuo*. The crude residue was purified by silica gel chromatography (pet. ether/ $CH_2Cl_2$, 8:2, *v/v*) to afford N,N-dibutyl-3-ethynylaniline as a yellow oil. 68%. $^1$H NMR (500 MHz, $CDCl_3$) δ [ppm] = 7.11 (t, 1H, CH $^3J$ = 10 Hz), 6.72-6.76 (m, CH, 3H), 6.61 (dd, 1H, CH, $^3J$ = 10 Hz, $^3J$ = 2.5 Hz), 3.25 (t, 4H, $CH_2$, $^3J$ = Hz), 1.53-157 (m, 4H, $CH_2$), 1.34-1.38 (m, 4H, $CH_2$), 0.97 (t, 6H, $CH_3$, $^3J$ = 10 HZ), 0.26 (s, 9H, $CH_3$). $^{13}$C NMR (126 MHz, $CDCl_3$) δ [ppm] = 147.9, 128.9, 123.5, 119.0, 114.8, 112.3, 106.4, 92.3, 50.6, 29.3, 20.3, 14.0, 0.0. ESI-HRMS: calcd for $C_{19}H_{32}NSi$: 302.2299 (M+H), found 302.2286 (M+H).

**N,N-dibutyl-3-ethynylaniline**: To a solution of N,N-dibutyl-3-trimethysilylethynylaniline (1 mmol) in a mixture of THF/MeOH (40 mL, 1:1, *v/v*) was added potassium fluoride (10 mmol) in portions. The mixture was heated at 50°C for 5 hours, before it was then taken up in $CH_2Cl_2$, washed with water three times, dried over $MgSO_4$ and concentrated *in vacuo*, to afford N,N-dibutyl-3-ethynylaniline, as a yellow oil. 92%. $^1$H NMR (500 MHz, $CDCl_3$) δ [ppm] = 7.14 (t, 1H, CH, $^3J$ = 10 Hz), 6.76-6.79 (m, CH, 3H), 6.64 (dd, 1H, CH, $^3J$ = 10 Hz, $^3J$ = 2.5 Hz), 3.26 (t, 4H, $CH_2$, $^3J$ = Hz), 3.01 (s, 1H, CH), 1.54-157 (m, 4H, $CH_2$), 1.33-1.40 (m, 4H, $CH_2$), 0.97 (t, 6H, $CH_3$, $^3J$ = 10 HZ). $^{13}$C NMR (126 MHz, $CDCl_3$) δ [ppm] = 148.0, 129.2, 123.6, 119.0, 115.0, 112.6, 85.0, 75.7, 50.7, 29.4, 20.4, 14.1. ESI-HRMS: calcd for $C_{16}H_{24}N$: 230.1903 (M+H), found 230.1893 (M+H).

**General procedures for salicylaldehyde derivatives 1a-1d**: To a solution of 4-bromosalicylaldehyde (1 mmol) and N,N-substituted-3 or 4-ethynylaniline (1.2 mmol) in a mixture of THF/$NEt_3$ (20 mL/5 mL) was added Pd(dppf)$Cl_2$ (0.05 mmol). The resulting mixture was degassed with Ar 30 minutes before CuI (0.1 mmol) were added. The mixture which turned rapidly black was stirred overnight at 60°C. The solution was then taken up in $CH_2Cl_2$, washed with water three times, dried over $MgSO_4$ and concentrated *in vacuo*. The crude residue was purified by silica gel chromatography (pet. ether/ $CH_2Cl_2$) to afford salicylaldehydes **1a-d** as a white to yellow oil or powders.

**Salicyladehyde 1a**. yellow oil. 78%. $^1$H NMR (500 MHz, $CDCl_3$) δ [ppm] = 11.09 (s, 1H, OH), 9.87 (s, 1H, CHO), 7.50 (d, 1H, $^3J$ = 10 Hz), 7.40 (dd, 2H, $^3J$ = 8 Hz, $^4J$ = 2.5 Hz), 7.09-7.13 (m, 2H), 6.60 (d, 2H, $^3J$ = 10 Hz), 3.32 (t, 4H, $CH_2$, $^3J$ = 8 Hz), 1.57-1.64 (m, 4H, $CH_2$), 1.34-1.43 (m, 4H, $CH_2$), 0.99 (t, 6H, $CH_3$, $^3J$ = 8 Hz). $^{13}$C NMR (126 MHz, $CDCl_3$) δ [ppm] = 197.1, 162.2, 149.8, 134.7, 134.2, 133.8, 123.3, 120.8, 119.5, 112.3, 108.1, 97.3, 87.7, 51.2, 20.9, 14.3. ESI-HRMS: calcd for $C_{23}H_{28}NO_2$: 350.2115 (M+H), found 350.2093 (M+H).

**Salicyladehyde 1b**. yellow powder. 53%. $^1$H NMR (500 MHz, $CDCl_3$) δ [ppm] = 11.05 (s, 1H, OH), 9.87 (s, 1H, CHO), 7.52 (d, 1H, $^3J$ = 10 Hz), 7.14-7.19 (m, 3H), 6.77-6.82 (m, 2H), 6.66 (dd, 1H, $^3J$ = 10 Hz, $^4J$ = 4 Hz), 3.27 (t, 4H, $CH_2$, $^3J$ = 10 Hz), 1.55-1.59 (m, 4H, $CH_2$), 1.35-1.39 (m, 4H, $CH_2$), 0.97 (t, 6H, $CH_3$, $^3J$ = 8 Hz). $^{13}$C NMR (126 MHz, $CDCl_3$) δ [ppm] = 195.8, 161.4, 148.1, 133.5, 132.5, 129.3, 123.1, 122.8, 120.3, 120.0, 118.9, 114.6, 112.9, 95.6, 87.2, 50.7, 29.4, 20.4, 14.1. ESI-HRMS: calcd for $C_{23}H_{28}NO_2$: 350.2115 (M+H), found 350.2096 (M+H).

**Salicyladehyde 1c**. white powder. 68%. $^1$H NMR (500 MHz, $CDCl_3$) δ [ppm] = 11.06 (s, 1H, OH), 9.88 (s, 1H, CHO), 7.49-7.52 (m, 3H), 7.11-7.14 (d, 2H, $^3J$ = 8 Hz), 6.90 (d, 2H, $^3J$ = 10 Hz), 3.84 (s, 3H, $CH_3$). $^{13}$C NMR (126 MHz, $CDCl_3$) δ [ppm] = 195.7, 161.4, 160.4, 133.6, 133.5, 132.5, 123.0, 120.1, 119.9, 114.4, 114.2, 94.4, 87.4, 55.4. ESI-HRMS: calcd for $C_{16}H_{13}O_3$: 253.0859 (M+H), found 253.0864 (M+H).

**Salicyladehyde 1d**. white powder. 58%. $^1$H NMR (500 MHz, $CDCl_3$) δ [ppm] = 11.05 (s, 1H, OH), 9.89 (s, 1H, CHO), 7.52-7.56 (m, 3H), 7.12-7.15 (m, 2H), 7.05-7.10 (m, 2H). $^{13}$C NMR (126 MHz, $CDCl_3$) δ [ppm] = 195.8, 164.3, 161.8, 161.4, 133.9, 133.5, 131.8, 123.0, 120.3, 120.1, 116.0, 115.8, 92.8, 88.1. ESI-HRMS: calcd for $C_{15}H_{10}FO_2$: 241.0659 (M+H), found 241.0646 (M+H).

**Salicyladehyde 2b**. yellow powder. 35%.$^1$H NMR (500 MHz, $CDCl_3$) δ [ppm] = 11.11 (s, 1H, OH), 9.84 (s, 1H, CHO), 7.48-7.52 (m, 3H), 7.22 (d, 1H, CH, $^3$J = 20 Hz), 7.14 (dd, 1H, CH, $^3$J = 10 Hz, $^4$J = 5 Hz), 7.07 (s, 1H, CH), 6.91-6.94 (m, 3H) 3.85 (s, 3H, $CH_3$). $^{13}$C NMR

(126 MHz, $CDCl_3$) δ [ppm] = 195.5, 162.1, 160.2, 147.0, 134.0, 132.9, 129.1, 128.5, 125.0, 119.6, 118.0, 114.5, 114.3, 55.4. ESI-HRMS calcd for $C_{16}H_{15}O_3$: 255.1016 (M+H), found 255.1024 (M+H).

**Salicyladehyde 3a**. yellow powder. 77%. $^1$H NMR (500 MHz, $CDCl_3$) δ [ppm] = 11.16 (s, 1H, OH), 9.84 (s, 1H, CHO), 7.56 (d, 2H, $^3$J = 10 Hz), 7.52 (d, 1H, $^3$J = 10 Hz), 7.23 (dd, 1H, $^3$J = 10 Hz, $^4$J = 2.5 Hz), 7.17 (s, 1H, CH), 6.74 (d, 2H, $^3$J = 10 Hz), 3.42 (q, 4H, $CH_2$, $^3$J = 10 Hz), 1.21 (t, 6H, $CH_3$, $^3$J = 10 Hz). $^{13}$C NMR (126 MHz, $CDCl_3$) δ [ppm] = 195.5, 162.2, 150.0, 148.4, 134.0, 128.4, 125.2, 118.5, 117.5, 113.5, 111.7, 44.5, 12.7. ESI-HRMS calcd for $C_{17}H_{20}NO_2$: 270.1489 (M+H), found 270.1499 (M+H).

**Salicyladehyde 3b**. white powder. 97%. $^1$H NMR (500 MHz, $CDCl_3$) δ [ppm] = 11.13 (s, 1H, OH), 9.90 (s, 1H, CHO), 7.58-7.60 (m, 3H), 7.23 (dd, 1H, $^3$J = 10 Hz, $^4$J = 2.5 Hz), 7.18 (s, 1H), 7.00 (d, 2H, $^3$J = 10 Hz), 3.87 (s, 3H, $CH_3$). $^{13}$C NMR (126 MHz, $CDCl_3$) δ [ppm] = 195.9, 162.0, 160.5, 149.5, 134.1, 131.7, 128.6, 119.2, 118.4, 115.1, 114.5, 55.4. ESI-HRMS calcd for $C_{14}H_{13}O_3$: 229.0859 (M+H), found 229.0867 (M+H).

## Photophysical properties in solution

The photophysical properties of salicylaldehyde derivatives **1a-1d**, **2a-b** and **3a-b** in solution are compiled in Table 1. All dyes were studied in toluene but dyes **1a**, **1b**, **2a** and **3a**, which demonstrated fluorosolvatochromic features, and were consequently studied in several solvents.

The absorption and emission of all dyes in toluene is presented on Figure 2, whereas those of salicylaldehydes **1a**, **2a** and **3a** in a wide range of solvents are presented on Figures 3a-3c respectively.

In toluene, salicyaldehydes **1a-d**, functionalized at the 4-position by ethynyl aryl groups with electrodonating ($NBu_2$, OMe) or withdrawing substituents (F) display maximum absorption wavelengths ($\lambda_{abs}$) in the 320-407 nm range with ε of 26200-31000 $M^{-1}.cm^{-1}$. A pronounced bathochromic shift is observed when the electronic density on the aryl side increases ($\lambda_{abs}$ **1a** > **1b** > **1c** >**1d**). This feature is also observed for the salicylaldehyde dyes **2a-b** and **3a-b** where the introduction of a dialkylamino moiety triggers the observation of a red-shifted absorption band, regardless of the nature of the spacer ($\lambda_{abs}$ = 425 and 367 nm for dyes **2a** and **2b**, respectively and $\lambda_{abs}$ = 392 and 321 nm for dyes **3a** and **3b**). The molar absorption coefficients remain, however in the same range (Figure 2a). Additional absorption bands are observed below 300 nm which can be assigned to $\pi$-$\pi^*$ transitions of the various conjugated

moieties of the dyes. In toluene, for all salicyaldehydes dyes **1a-1d**, **2a** and **3a-b**, a sizeable emission band is observed after photoexcitation in the lowest energy band ($\lambda_{exc}$ = 310-420 nm). A notable exception is **2b** which is non-fluorescent. Luminescent lifetimes recorded are in the nanosecond range, which is typically expected for purely organic fluorophores.

**Table 1**. Photophysical data for salicylaldehyde dyes **1a-1d, 2a-b** and **3a-b** recorded in aerated solutions at 25°C.

| Dye | $\lambda_{abs}$ (nm) | ε ($M^{-1}.cm^{-1}$) | $\lambda_{em}$ (nm) | ΔS ($cm^{-1}$)[b] | $\Phi_F$[a] | τ (ns) | $K_r$[c] | $K_{nr}$[c] | Solvent |
|---|---|---|---|---|---|---|---|---|---|
| **1a** | 412 | 33000 | 424 | 690 | 0.53 | 1.3 | 4.08 | 3.62 | CH[d] |
| **1a** | 407 | 31000 | 490 | 4200 | 0.68 | 3.1 | 2.19 | 1.03 | toluene |
| **1a** | 398 | 42300 | 508 | 5400 | 0.60 | 3.4 | 1.76 | 1.18 | $Et_2O$ |
| **1a** | 401 | 33000 | 555 | 6900 | 0.11 | 2.5 | 0.44 | 3.56 | THF |
| **1a** | 411 | 38000 | 605 | 7800 | 0.02 | 0.6 | 0.33 | 16.30 | $CH_2Cl_2$ |
| **1a** | 351 | 11600 | 533 | 9700 | 0.01 | 0.4 | 0.25 | 24.80 | $CH_2Cl_2/H^+$ |
| **1a** | 400 | 30800 | [e] | [e] | [e] | [e] | [e] | [e] | Acetone |
| **1a** | 400 | 27000 | [e] | [e] | [e] | [e] | [e] | [e] | $CH_3CN$ |
| **1a** | 401 | 25500 | 442/594 | 2300 | 0.01 | 0.5 | 0.20 | 19,80 | DMSO |
| **1a** | 400 | 30400 | 587 | 8000 | 0.02 | 0.4 | 0,50 | 24,50 | DMF |
| **1b** | 393 | 25100 | 445 | 3000 | 0.12 | 2.3 | 0.53 | 3.83 | CH[d] |
| **1b** | 388 | 26200 | 506 | 6000 | 0.29 | 10.0 | 0.29 | 0.71 | toluene |
| **1b** | 389 | 25400 | 410/605 | 9200 | 0.06 | 4.1 | 0.15 | 2.29 | THF |
| **1b** | 394 | 28300 | 654 | 10100 | 0.02 | 1.7 | 0.12 | 5.76 | $CH_2Cl_2$ |
| **1b** | 348 | 34100 | 533 | 10000 | 0.01 | 0.8 | 0.13 | 12.40 | $CH_2Cl_2/H^+$ |
| **1c** | 346 | 26800 | 424/532 | 5300 | 0.01 | 0.5 | 0.20 | 19.80 | toluene |
| **1d** | 320 | 30300 | 411/533 | 12500 | 0.01 | 0.4 | 0.25 | 24.80 | toluene |
| **2a** | 416 | 31000 | 423 | 3980 | 0.04 | 0.4 | 1.00 | 24.00 | CH[d] |
| **2a** | 425 | 26000 | 508 | 3800 | 0.10 | 0.8 | 1.25 | 11.30 | toluene |
| **2a** | 415 | 15200 | 522 | 4900 | 0.19 | 0.8 | 2.38 | 10.10 | $Et_2O$ |
| **2a** | 425 | 31000 | 558 | 5600 | 0.29 | 1.6 | 1.81 | 4.44 | THF |
| **2a** | 436 | 25800 | 593 | 6100 | 0.64 | 2.2 | 2.91 | 1.64 | $CH_2Cl_2$ |
| **2a** | 331 | 20600 | 418/532 | 6300 | 0.04 | 0.4 | 1.00 | 24.00 | $CH_2Cl_2/H^+$ |
| **2a** | 425 | 30000 | 600 | 6900 | 0.44 | 2.4 | 1.83 | 2.33 | Acetone |
| **2a** | 427 | 28600 | 631 | 7600 | 0.47 | 2.0 | 2.35 | 2.65 | $CH_3CN$ |
| **2a** | 426 | 26400 | 643 | 7900 | 0.09 | 0.5 | 1.80 | 18.20 | EtOH |
| **2a** | 425 | 27000 | 602 | 6900 | 0.22 | 2.4 | 0.92 | 3.25 | DMSO |
| **2a** | 430 | 26200 | 617 | 7100 | 0.70 | 2.4 | 2.92 | 1.25 | DMF |
| **2b** | 367 | 35700 | [e] | [e] | [e] | [e] | [e] | [e] | toluene |
| **3a** | 383 | 50400 | 410/568 | 1700 | 0.24 | 0.2 | 12.0 | 38.0 | CH[d] |
| **3a** | 392 | 30100 | 459 | 3700 | 0.48 | 1.3 | 3.69 | 4.00 | toluene |
| **3a** | 383 | 31800 | 464 | 4600 | 0.38 | 2.1 | 1.81 | 2.95 | $Et_2O$ |
| **3a** | 389 | 18200 | 504 | 5900 | 0.76 | 2.4 | 3.17 | 1.00 | THF |
| **3a** | 396 | 32200 | 532 | 6500 | 0.56 | 2.3 | 2.43 | 1.91 | $CH_2Cl_2$ |
| **3a** | 332 | 7800 | [e] | [e] | [e] | [e] | [e] | [e] | $CH_2Cl_2/H^+$ |
| **3a** | 391 | 69800 | 548 | 7300 | 0.09 | 0.5 | 1.80 | 18.20 | Acetone |
| **3a** | 387 | 27200 | 546 | 7500 | 0.03 | 0.2 | 1.50 | 48.50 | EtOH |
| **3a** | 390 | 26800 | 533 | 6900 | 0.58 | 3.0 | 1.93 | 1.40 | DMSO |
| **3a** | 385 | 27800 | 520 | 6700 | 0.27 | 2.9 | 0.93 | 2.52 | DMF |
| **3b** | 321 | 29800 | 400/527 | 6200 | 0.01 | 0.2 | 0.10 | 49.50 | toluene |

[a] Relative quantum yield determined in solution using Rhodamine 6G as a reference ($\lambda_{exc}$ = 488 nm, Φ = 0.88 in ethanol), [b] Stokes shift, [c] $k_r$ ($10^8$ $s^{-1}$) and $k_{nr}$ ($10^8$ $s^{-1}$) were calculated using: $k_r = \Phi_F/\sigma$, $k_{nr} = (1- \Phi_F)/\sigma$ where σ is the lifetime, [d] Cyclohexane [e] Non fluorescent.

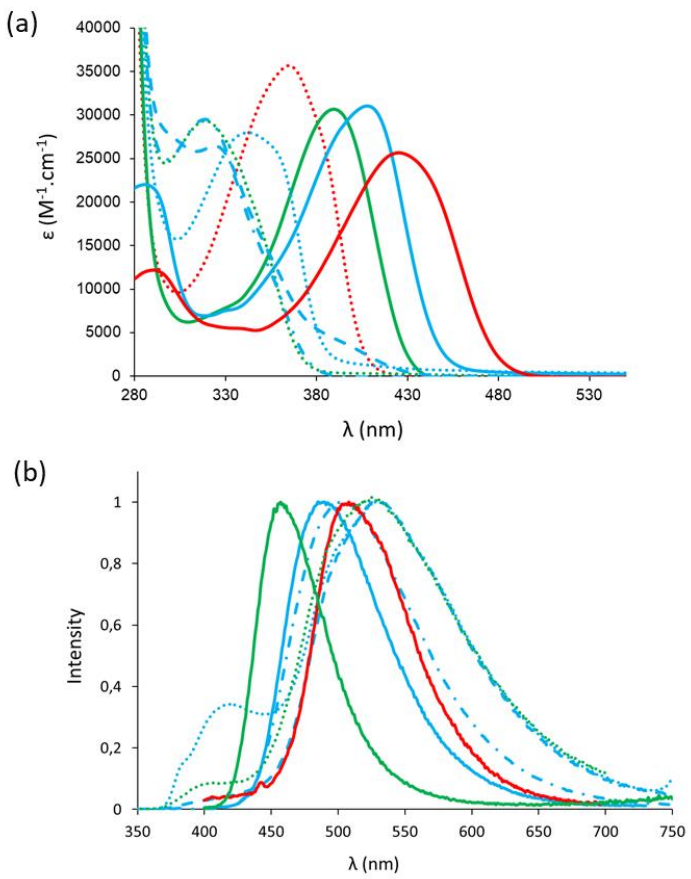


**Figure 2.** (a) UV-Vis. and (b) Emission spectra of salicylaldehyde **1a** (plain blue), **1b** (dotted blue), **1c** (dashed blue), **1d** (dotted dashed blue), **2a** (plain red), **2b** (dotted red), **3a** (plain green) and **3b** (dotted green) in aerated solutions of toluene at room temperature.

In toluene, salicyaldehydes **1a-d**, functionalized with an ethynyl-extended spacer at the 4 position display a single or a dual emission band in the range 424-533 nm. Two types of photophysical behaviors can be clearly evidenced: **1a** and **1b**, bearing a meta- or para-substituted N,N-dibutylamino group feature a single emission band ($\lambda_{em}$ = 490 and 506 nm for **1a** and **1b**, respectively) whereas **1c** and **1c**, incorporating a para-substituted methoxy or fluoro group show a dual emission profile ($\lambda_{em}$ = 424/532 nm and 411/533 nm for **1c** and **1d**, respectively). The intense emission band observed in the case of **1a** and **1b** can ascribed to the sole presence of the excited enol tautomer $E^*$, as a result of a complete frustration of the ESIPT process. This phenomenon was previously observed on other π-extended ESIPT emitters and was rationalized by the occurrence of a $S_1$-$S_0$ transition delocalized over the conjugated spacer.[24] This assumption can be further confirmed by the strong values of the calculated quantum yields in toluene (Φ = 0.68 and 0.29 for **1a** and **1b**, respectively),

indicative of a lack of ESIPT process, and is also consistent with theoretical modelling (*vide infra*). As for **1c** and **1d** are concerned, a dual emission is observed in toluene with a second band being much more intense than the first one (in the case of **1d**, the intensity of $E^*$ is very weak). Moreover, a strong bathochromic shift for the main emission band, as compared to that of **1a** and **1b** ($\lambda_{em}$ =532 and 533 nm for **1c** and **1d**, respectively). This optical behavior clearly emphasizes a partial frustration of ESIPT, translating into the observation of a dual $E^*$/Keto ($K^*$) process. The $K^*$ tautomer generated by ESIPT being is predominant in the excited-state explaining the very low quantum yield ($\Phi$ = 0.01 for both **1c** and **1d**); a feature consistent with the detrimental molecular motions induced by the proton transfer in the excited-state, leading to more efficient non-radiative deactivations pathways. The electronic nature of the functional group present on the core of the aryl group ($NBu_2$ *vs.* OMe or F) clearly influences the $pKa^*$ of the phenol moiety and subsequently the efficiency of the ESIPT process. Salicyaldehydes **2a-b** and **3a-b** seem to follow the same trends. Indeed, dyes **2a** and **3a**, both functionalized by a strongly electrodonating *N*,*N*-dialkylamino moiety at the para position of the aryl ring display intense $K^*$ single emission bands at 508 and 459 nm, respectively. Meanwhile, dye **2b** appears to be non-emissive and dye **3b** shows a faint dual $E^*/K^*$ emission ($\lambda_{em}$ =400/527 nm, $\Phi$ = 0.01 in toluene).

Intrigued by the bright emission recorded for the salicylaldehyde derivatives functionalized by an aromatic amine group, *i.e.* **1a-b**, **2a** and **3a**, regardless of the nature of the spacer, we decided to investigate their photophysical properties in a range of solvents with increasing dielectric constants (Figures 3a-c). First, the maximum absorption wavelength for each dye does not significantly change upon increase of the dipole moment of the solvent ($\lambda_{abs}$ = 398-412 nm for **1a**, $\lambda_{abs}$ = 388-394 nm for **1b**, $\lambda_{abs}$ = 415-430 nm for **2a**, $\lambda_{abs}$ = 383-396 nm for **3a**), highlighting a moderately polarized ground state.

In the excited-state, however, sizeable differences can be evidenced between dyes **1a**, **2a**, and **3a**, evidencing a pronounced influence of the nature of the $\pi$-conjugated spacer on the emissive properties. Ethynyl-extended salicylaldehyde **1a** displays characteristic features of strong fluorosolvatochromism, *i.e.*, the observation of a gradual bathochromic shift upon increase of the dielectric constant of the solvent. In apolar medium, *i.e.*, cyclohexane, toluene, diethylether or THF, a strong single red-shifting emission band is observed ($\lambda_{em}$ = 424-555 nm) with a high quantum yield ($\Phi$ = 0.11-0.68). However, in polar media (dichloromethane, acetone, acetonitrile, DMSO and DMF), fluorescence appears to be significantly quenched ($\lambda_{em}$ = 587-605 nm, $\Phi$ = 0.01-0.02). Similar fluorosolvatochromism behaviors are observed for dyes **2a** and **3a** with a weaker intensity. Indeed, in the case of **2a** functionalized with a

vinyl extended spacer, a strong fluorescence intensity is found in most of the solvents studied with a maximum emission wavelength spanning the entire visible spectrum ($\lambda_{em}$ = 423-643 nm, $\Phi$ = 0.04-0.70). Unlike **1a**, the fluorescence quantum yield of **2a** seems to significantly increase along with the dielectric constant of the solvent, from 0.04 in cyclohexane to 0.70 in DMF. As reported in the literature on similar dyes whose excited-state possesses a charge transfer character, solvent polarity tends to strongly interfere with the photoisomerisation process of the vinyl spacer, with a stronger photoisomerisation efficiency in apolar media.[25]

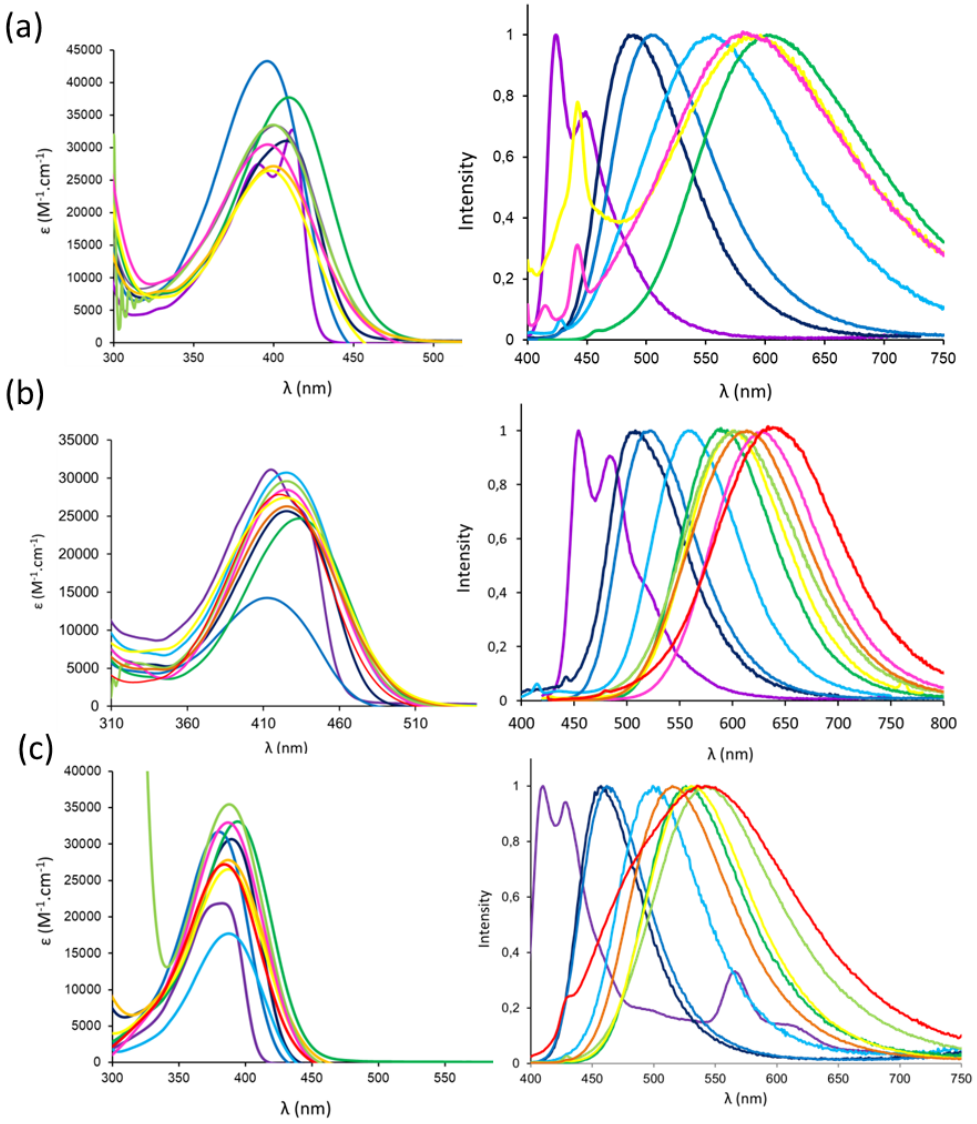


**Figure 3.** Absorption (left) and emission (right) of salicylaldehydes (a) **1a**, (b) **2a** and (c) **3a** in cyclohexane (purple), toluene (navy blue), diethyl ether (blue), THF (light blue), dichloromethane (green), acetone (light green), acetonitrile (orange), DMSO (yellow), DMF (pink) and ethanol (red).

Dye **3a**, where the aryl group is directly functionalized onto the salicylaldehyde core similarly displays a strong charge transfer character with a maximum emission wavelength spanning from 410 to 560 nm with quantum yields in the range 0.03-0.76.

Protonation studies were performed by bubbling HCl gas into a dichloromethane solution of dyes **1a-b**, **2a** and **3b**, bearing protonable N,N-dialkylamino groups. In all cases, the protonation led to strongly blue-shifted absorption and emission bands, along with a strong quenching of fluorescence intensity. This trend is particularly noticeable for dye **2a** ($\lambda_{abs}$/ $\lambda_{em}$ = 436/593 nm vs. 331/532 nm in neutral and protonated dichloromethane, respectively) with a quantum yield dropping from 0.64 to 0.04.

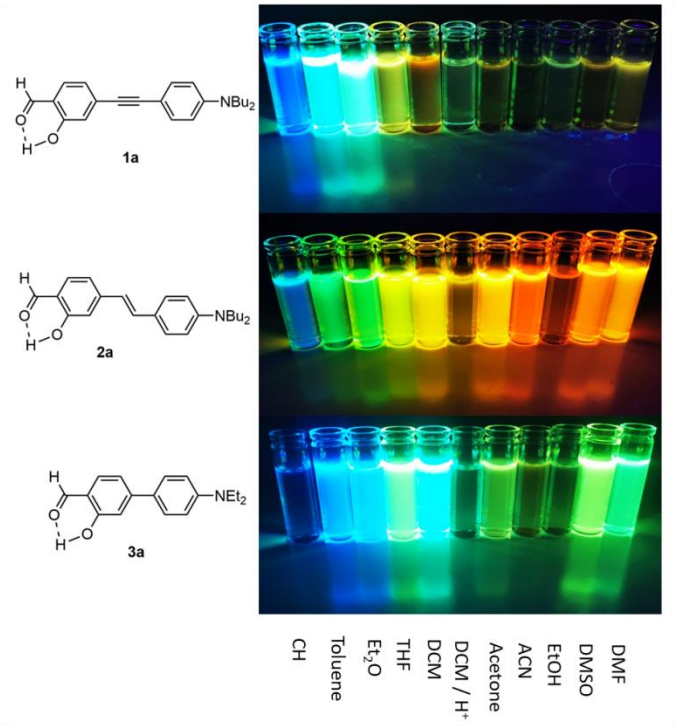


**Figure 4.** Photographs under irradiation ($\lambda_{exc}$ = 365 nm) of salicylaldehyde **1a** (top), **2a** (middle) and **3a** (bottom) in solution (from left to right: cyclohexane, toluene, diethylether, THF, dichloromethane, protonated dichloromethane, acetone, acetonitrile, ethanol, DMSO and DMF).

The photophysical behavior observed for all dyes substituted with N,N-dialkylamino groups is characteristic of the presence of a strong internal charge transfer (ICT) process in the excited-state where dipole moments of the excited molecules align with those of the solvent to provide highly polarized solvated excited species. To ascertain the charge transfer nature of the excited-state, Lippert-Mataga curves were plotted for dyes **1a**, **2a** and **3a** (Figure S2.40).

The dipole moment differences between the excited and ground states (Δμ) were calculated to reach 25.6, 21.7 and 22.3D for dyes **1a**, **2a** and **3a**, respectively, which are in the highest range of values for similar fluorosolvatochromic emitters, highlighting a highly polarized excited-state.[26] To illustrate the strong impact of the solvent in the emission color and intensity, Figure 4 represents photographs of dyes **1a**, **2a** and **3a** in solution in different solvents under irradiation with a UV-bench lamp ($\lambda_{exc}$ = 365 nm).

## Viscosity-induced fluorescence enhancement

The intensity of the emission of dye **3a**, which features a direct connection between the two aryl rings appears to be higher in polar solvents with higher polarities such as DMSO ($\lambda_{em}$ = 533 nm, Φ = 0.58). This prompted us to explore the viscosity-induced fluorescence enhancement in different mixtures of EtOH/glycerol (1:0 to 1:9) (Figure 5). Viscosity molecular probes which often feature donor-acceptor rotor-shaped dyes and display twisted intramolecular charge transfer (TICT) can be advantageously applied in many sensing applications.[27]

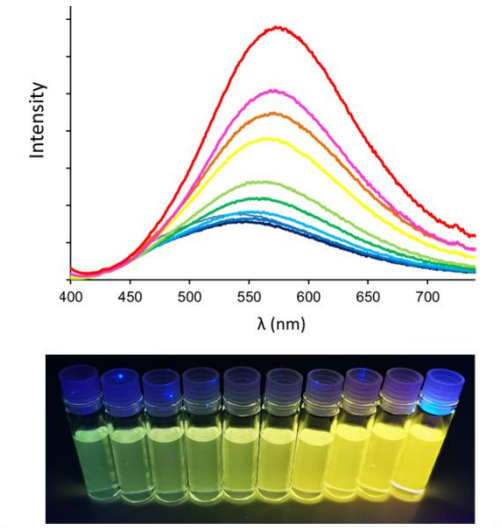


**Figure 5.** (top) Emission spectra of salicylaldehyde **3a** in ethanol/glycerol mixtures from EtOH (100%) to EtOH/glycerol (90/10). (bottom) Photographs of solutions of **3b** in ethanol/glycerol mixtures under irradiation from a UV bench lamp ($\lambda_{exc}$ = 365 nm).

Upon increasing the solution viscosity, a strong fluorescence enhancement can be clearly detected by the naked eye. The maximum emission gradually shifts from 546 to 575 nm with an approximate 5-fold enhancement when going from pure ethanol to a 1:9 mixture with

glycerol. This viscosity effect, which remains mild as compared to reported viscosity sensors,[27] can be attributed to the restriction of rotation between the electron donating aryl group and the salicyladehyde on the one hand and the rotation between the dialkylamino moiety and the aryl group on the other hand, in high viscosity media.

## Solid-state emission

Salicyaldehyde **1a-b**, **2a** and **3a** show significant fluorescence emission by the naked eye as amorphous powders or oils under irradiation from UV bench lamp ($\lambda_{exc}$ = 365 nm). The fluorescence emission was recorded, as 10% wt doped in poly(methylmethacrylate) (PMMA) films. The photophysical data can be found on Table S2 and Figure 6. The maximum emission wavelength is centered on 400 nm, with the exception of dye **2b** which shows a red-shifted emission at 428 nm. The quantum yields, calculated as absolute values range from 0.44 to 0.88, evidencing these dyes as dual-state emitters.

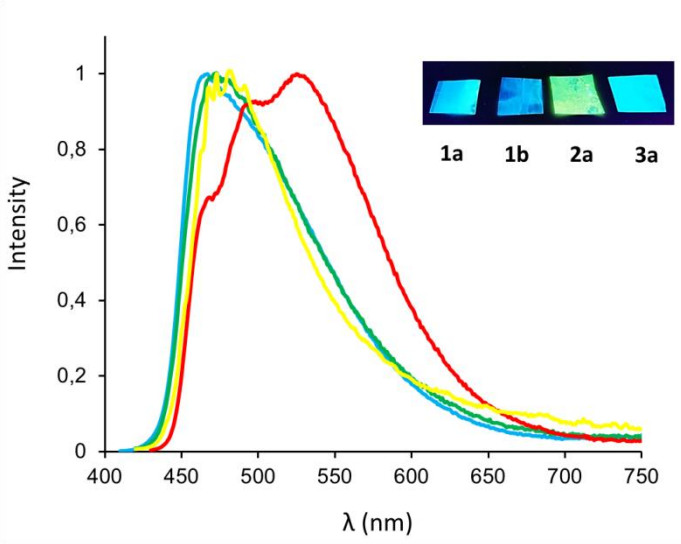


**Figure 6.** Emission spectra of salicylaldehyde **1a** (blue), **1b** (green), **2a** (red) and **3a** (yellow) as 10% *wt* doped in poly(methylmethacrylate) (PMMA) films. Insert: photographs of the PMMA films under irradiation ($\lambda_{exc}$ = 365 nm).

## First-principle calculations

To obtain a complementary view on the nature of the emitting species of the synthesized salicyaldehydes, theoretical calculations have been performed using an *ab initio* approach detailed in the SI. During the calculations, the long alkyl chains have been replaced by Me groups for the sake of computational efficiency. The main theoretical results are collected in Table 2. First, for absorption, one can note that all theoretical values are slightly blue-shifted (by *ca*. 20 nm) as compared to the experimental values, which is attributed to the neglect of vibronic effects in the calculation. The trends are however, nicely reproduced, *i.e.* the dyes yielding the most red-shifted absorption bands being salicylaldehydes **1a**, **2a** and **3a**, as in the measurements (Tables 1 and 2).

**Table 2.** Computed vertical absorption, enol and keto vertical emission wavelengths together with the free energy difference between the enol and keto forms ($\Delta G^{E^*-K^*}$), the predicted origin of the emission and the excited-state dipole moments of the two forms. See the SI for details regarding the selected theoretical approach.

| Dye | $\lambda_{abs}$ (nm) | $\lambda_{em}$ (E*) (nm) | $\lambda_{em}$ (K*) (nm) | $\Delta G^{E^*-K^*}$ (eV) | Predicted emission | $\mu$ (E*) (D) | $\mu$ (K*) (D) | Solvent |
|---|---|---|---|---|---|---|---|---|
| **1a** | 380 | 431 | [b] | [b] | E* | 22.4 | [b] | toluene |
| **1b** | 361 | 426 | 466 | +0.28 | E* | 22.6 | 7.3 | toluene |
| **1c** | 336 | 379 | 466 | -0.10 | Dual | 15.6 | 6.9 | toluene |
| **1d** | 336 | 364 | 466 | -0.24 | K* | 8.6 | 4.4 | toluene |
| **2a** | 407 | 476 | [b] | [b] | E* | 20.2 | [b] | toluene |
| **2b** | 351 | 418 | 459 | +0.19 | E* | 14.5 | 7.2 | toluene |
| **3a** | 365 | 416 | 479 | +0.28 | E* | 18.9 | 13.1 | toluene |
| **3b**[a] | 343 | 369 | 469 | -0.08 | Dual | 12.2 | 6.9 | toluene |

[a] Corresponding to the second state, the first transition is nearly dark for E*, see text. [b] K* form unfound in the excited-state.

The predicted features for the fluorescence are nicely in line with the experimental ones. For salicyaldehyde **1a**, which is a strong ICT dye, theory predicts that the $K^*$ tautomer does not exist (optimizations starting from this structure yield back $E^*$). The emission is thus originating solely from $E^*$, which is consistent with the experimental findings (very large quantum yield). Interestingly both the computed Stokes shift (3113 $cm^{-1}$) and excited-state dipole (22.4 D corresponding to a $\Delta\mu$=13.2 D) agree quite well with the experimental findings (4200 $cm^{-1}$ and 25.6 D, respectively).

In the meta-substituted salicylaldehyde **1b**, a very swallow $K^*$ minimum could be located but it appears much less stable than its $E^*$ counterpart, so there is no ESIPT driving force and only $E^*$ fluorescence should be observed. This is also fitting the experimental photophysical measurements characterized by a large emission quantum yield and a large, yet not huge Stokes shift. If one decreases the strength of the donor group (**1c**), the two tautomers become almost isoenergetic with a slight driving force of -0.10 eV for the ESIPT process. Such value is typical of dual emitters,[28] which fits indeed the experimental observation in toluene (Figure 2) and with the observed small quantum yield. Note that the computed $E^*$ emission of salicylaldehyde **1a** falls in between the $E^*$ and $K^*$ emissions of **1c** according to theory, again matching the experimental trends. In going to **1d**, one now obtains a clearly more stabilized $K^*$ structure which should solely emit. This is what is found experimentally (although a very weak residual $E^*$ emission can be detected in Figure 2). We note that the enol excited states in **1c** and **1d** are much less polar than in **1a** and **1b**, confirming that the ICT is much larger in the two latter dyes.

In the vinyl series, salicylaldehyde **2a** behaves similarly as **1a** according to the calculation: only the enol emission can be observed and the excited state of **2a** is very polarized, though slightly less than in **1a**. This fits well the observations of a significant Stokes shift, non-negligible quantum yields and strong solvatofluorochromism. In contrast **2b** departs from the behavior of the homologous **1c**, according to theory. Indeed in **2b**, theory foresees that the formation of the $K^*$ structure would be uphill by +0.19 eV, *i.e.*, that a sole $E^*$ emission should be observed. However, experimentally **2b** is non-emissive, maybe due to isomerization around the double bond, making comparisons impossible.

As for the directly bonded salicylaldehydes **3a-b**, unsurprisingly, **3a** behaves like **1a** and **2a**, *i.e.* the keto form is too unstable to exist and a single fluorescence band stemming from the enol characterized by a strong ICT nature is predicted by the calculations; again perfectly fitting the experimental observations. Salicylaldehyde **3b** is more specific, *i.e.* it is the sole dye of the series for which theory predicts that the lowest absorption transition is associated to a small oscillator strength. The optimization of this state leads to a dark state, which should be non-emissive due to a trifling $K_r$. If one starts the optimization process from the second (brighter state), one obtains a typical dual emission from both tautomers as the ESIPT driving force is moderate (-0.08 eV). Therefore, the photophysical properties of **3b** can be explained by the fact that the absorption to the strongly dipole-allowed $S_2$, is followed by a competition between ESIPT, leading directly to the $S_1$ of $K^*$ and a weak emission, or internal conversion to the $S_1$ of $E^*$ which relaxes non-radiatively (dark state quenching). In the experimental graph

of Figure 2b, there is a small blue-shifted emission band, likely coming from a (non-Kasha but very limited) residual $S_2$ of $E^*$ emission.

## Conclusion

In conclusion, a series of original π-extended salicylaldehyde dyes functionalized by electron donating or withdrawing groups and various spacers have been synthesized and characterized spectroscopically in solution and in the solid-state. The nature of the spacer has a strong influence on the nature of the excited-states, *i.e.* the quantitative, partial or absence of ESIPT process. All experimental results have been rationalized by first-principle calculations. Owing to their strong environment-sensitive emission profile, these dyes appear to be attractive candidates for sensing applications. Work along these lines are currently in progress.

## Acknowledgments

The authors thank the CNRS and the ANR for support in the framework of the GeDeMi grant D.J. thanks the CCIPL (*Centre de Calcul Intensif des Pays de la Loire*) installed in Nantes for generous allocation of computational time. T.S acknowledges the ministère de l'enseignement supérieur, de la recherche et de l'innovation for a PhD fellowship.

## References

(1) (a) X. Tian, L.C. Murfin, L. Wu, S.E. Lewis, T.D. James, *Chem. Soc. Rev*., **2021**, DOI: 10.1039/d0sc06928k. (b) (b) M. Gao, F. Yu, C. Lv, J. Choo, L. Chen, *Chem. Soc. Rev*., **2017**, 46, 2237-2271. (c) G. Hong, A.L. Antaris, H. Dai, *Nat. Biomed. Eng*., **2017**, 1,1, 010. (d) M. Gsänger , D. Bialas , L. Huang , M. Stolte , F. Würthner, *Adv. Mater*., **2016**, *28*, 3615-3645.
(2) (a) A.P. Gorka, R.R. Nani, M. J. Schnermann, *Acc. Chem. Res*., **2018**, 51, 3226-3235. (b) M. Panigrahi, S. Dash, S. Patel, B.K. Mishra, *Tetrahedron*, **2012**, 68, 781-805. (c) B. Le Guennic, D. Jacquemin, *Acc. Chem. Res*., **2015**, 48, 530-537.
(3) (a) A.S. Klymchenko, *Acc. Chem. Res*., **2017**, 50, 2, 366-375. (b) Y.M. Poronik, K.V. Vygranenko, D. Gryko, D.T. Gryko, *Chem. Soc. Rev*., **2019**, 48, 5242-5265.
(4) (a) S. Khopkar, G. Shankarling, *Dyes & Pigm*., **2019**, 170, 107645. (b) D. E. Lynch, D.G. Hamilton, *Eur. J. Org. Chem*., **2017**, 3897-3911.

(5) (a) D. Frath, J. Massue, G. Ulrich, R. Ziessel, R. *Angew. Chem., Int. Ed*. **2014**, 53, 2290-2310. (b) G. Ulrich, R. Ziessel, A. Harriman, *Angew. Chem., Int. Ed.* **2008**, 47, 1184-1207. (c) J. Taguchi, S. Matsuura, T. Seki, H. Ito, *Chem. Eur. J*., **2020**, 26, 2450-2455.

(6) (a) J. Mei, N.L.C. Leung, R.T.K. Kwok, J. W. Y. Lam, B.Z. Tang, *Chem. Rev*., **2015**, 115, 11718-11740. (b) W. Xu, D. Wang, B. Zhong Tang, *Angew. Chem., Int. Ed*. **2021**, DOI: 10.1002/anie.202005899.

(7) (a) A. Raghuvanshi, A.K. Jha, A. Sharma, S. Umar, S. Mishra, R. Kant, A. Goel, *Chem. Eur. J*. **2017**, 23, 4527-4531. (b) Q. Qiu, P. Xu, Y. Zhu, J. Yu, M. Wei, W. Xi, H. feng, J. Chen, Z. Qian, *Chem. Eur. J*., **2019**, 25, 15983-15987.

(8) K. Skonieczny, J. Yoo, J.M. Larsen, E.M. Espinoza, M. Barbasiewicz, V.I. Vullev, C.-H. Lee, D.T. Gryko, *Chem. Eur. J.* **2016**, 22, 7485-7496.

(9) N. Suzuki, K. Suda, D. Yokogawa, H. Kitoh-Nishioka, S. Irle, A. Ando, L.M.G. Abegão, K. Kamada, A. Fukazawa, S. Yamaguchi, *Chem. Sci*., **2018**, 9, 2666-2673.

(10) (a) K. Takagi, K. Ito, Y. Yamada, T. Nakashima, R. Fukuda, M. Ehara, H. Masu, *J. Org. Chem.* **2017**, 82, 12173-12180. (b) T. Pariat, M. Munch, M. Durko-Maciag, J. Mysliwiec, P. Retailleau, P. M. Vérité, D. Jacquemin, J. Massue, G. Ulrich, *Chem. Eur. J*., **2021**, 27, 10, 3483-3495.

(11) (a) Y.-H. Hsu, Y.-A. Chen, H.-W. Tseng, Z. Zhang, J.-Y. Shen, W.-T. Chuang, T.-C. Lin, C.-S. Lee, B.-C. Hong, S.-H. Liu, P.-T. Chou, *J. Am. Chem. Soc*., **2014**, 136, 11805-11812. (b) H. Wu, Z. Chen, W. Chi, B.A. Kaur, L. Gu, C. Qian, B. Wu, B. Yue, G. Liu, G. Yang, L. Zhu, Y. Zhao, *Angew. Chem., Int. Ed*., **2019**, 58, 33, 11419-11423. (c) A. Goel, A. Sharma, M. Rawat, R.S. Anand, R. Kant, *J. Org. Chem*. **2014**, 79, 10873-10880.

(12) (a) D. Frath, K. Benelhadj, M. Munch, J. Massue, G. Ulrich, *J. Org. Chem*. **2016**, 81, 9658-9668. (b) F. Zhao, J. Tian, X. Wu, S. Li, Y. Chen, S. Yu, X. Yu, L. Pu, *J. Org. Chem*. **2020**, 85, 7342-7348.

(13) (a) P. Yadav, M. Jakubaszek, B. Spingler, B. Goud, G. Gasser, F. Zelder, *Chem. Eur. J*., **2020**, 26, 5717-5723. (b) L. Zhou, Y. Feng, J. Cheng, N. Sun, X. Zhou, H. Xiang, *RSC Adv*., **2012**, 2, 10529-10536.

(14) (a) A. Karawek, P. Mayurachayakul, T. Santiwat, M. Sukwattanasinitt, N. Niamnont, *J. Photobiol. Photochem., A: Chemistry*, **2021**, 404, 112879. (b) W.-H. Hong, C.-C. Lin, T.-S. Hsieh, C.-C. Chang, *Dyes & Pigm*., **2012**, 94, 371-379.

(15) Y.-J. Zhuang, J.-P. Qu,Y.-B. Kang, *J. Org. Chem*., **2020**, 85, 4386-4397.

(16) (a) M. Yamajia, H. Okamoto, *J. Photochem. Photobiol. A: Chemistry*, **2018**, 360, 204-209. (b) P.A.A.M. Vaz, J. Rocha, A.M.S. Silva, S. Guieu, *Dyes & Pigm*., **2021**, 184, 108720.

(17) (a) S. Zhang, J. Tang, J. Zhang, F. Xu, S. Chen, D. Hu, B. Yin, J. Zhang, *Inorg. Chem*., **2021**, 60, 816-830. (b) S. Arumugam, B. Shankar, K.C. Mondal, *Eur. J. Inorg. Chem*., **2020**, 4127-4136.

(18) H.A. Rudbari, F. Lloret, M. Khorshidifard, G. Bruno, M. Julve, *RSC Adv*., **2016**, 6, 7189-7194.

(19) (a) J. Massue, D. Jacquemin, G. Ulrich, *Chem. Lett*., **2018**, 47, 9, 1083-1089. (b) J. Zhao, S. Ji, Y. Chen, H. Guo, P. Yang, *Phys. Chem. Chem. Phys*. **2012**, 14, 8803-8817. (c) V.R. Mishra, C.W. Ghanavatkar, N. Sekar, *ChemistrySelect*, **2020**, 5, 2103-2113. (d) V.S. Padalkar, S. Seki, *Chem. Soc. Rev*. **2016**, 45, 169-202.

(20) (a) K. Benelhadj, W. Muzuzu, J. Massue, P. Retailleau, A. Charaf-Eddin, A.D. Laurent, D. Jacquemin, G. Ulrich, R. Ziessel, *Chem. Eur. J*., **2014**, 20, 12843-12857. (b) E. Heyer, K. Benelhadj, S. Budzák, D. Jacquemin, J. Massue, G. Ulrich, *Chem. Eur. J*. **2017**, 23, 7324-7336.

(21) K. Tahara, T. Fujita, M. Sonoda, M. Shiro, Y. Tobe, *J. Am. Chem. Soc*., **2008**, 130, 43, 14339-14345.

(22) A.-P. Xuac, H.-H. Han, J. Lu, P.-P. Yang, Y.-J. Gao, H.-W. An, D. Zhanng, L.-Z. Li, J.-P. Zhang, D. Wang, L. Wang, H. Wang, *Dyes & Pigm*., **2016**, 125, 392-398.

(23) D. Frath, P. Didier, Y. Mély, J. Massue, G. Ulrich, *ChemPhotoChem*.**, 2017,** 1, 109-112.

(24) M. Raoui, J. Massue, C. Azarias, D. Jacquemin, G. Ulrich, *Chem. Commun*. **2016**, 52, 9216-9219.

(25) M. Mac, A. Danel, T. Uchacz, S. Gorycka, K. Gorz, S. Lesniewski, E. Kulig, *Photochem. Photobiol. Sci.*, **2010**, 9, 357-364.

(26) S. Y. Fung, J. Duhamel, P. Chen, *J. Phys. Chem. A*, **2006**, 110, 11446-11454.

(27) (a) P. R. Aswathy, S. Sharma, N. P. Tripathi, S. Sengupta, *Chem. Eur. J*., **2019**, 25, 14870-14880. (b) B. Sk, S. Khodia, A. Patra, *Chem. Commun*., **2018**, 54, 1786-1788.

(28) C. Azarias, S. Budzak, A. D. Laurent, G. Ulrich, D. Jacquemin, *Chem. Sci*. **2016**, 7, 3763–3774